THE JOURNAL OF PHYSICAL CHEMISTRY B

Article

pubs.acs.org/JPCB

# Reversible Adsorption−Desorption Oscillations of Nanoparticles on a Patterned Hydrogel Surface Induced by a pH Oscillator in a Closed Chemical System

Jin Kyung Kim,[†] Kwang Il Kim,[†] C. Basavaraja,[†] G. Rabai,[‡] and Do Sung Huh*[,†]

[†]Department of Chemistry, Inje University, Obang 607, Gimhae City, South Korea

[‡]Institute of Physical Chemistry, University of Debrecen, P.O. Box 7.H-4010 Debrecen, Hungary

**ABSTRACT:** Oscillatory adsorption−desorption of Ag nanoparticles on a pH-responsive hydrogel surface was induced by a pH oscillator in a closed reaction system. The hydrogel surface was prepared as a honeycomb-patterned film using a honeycomb-patterned polystyrene film as a template to speed up the response time in the stimuli-responsive hydrogel. The surface morphology and hydrophobic interaction of the patterned hydrogel surface were significantly altered by the pH change of the aqueous solution that came into contact with the gel. The surface of the hydrogel became hydrophobic for adsorption in a lower-pH solution but became hydrophilic with decreased adsorptivity at higher pH conditions. A closed system chemical pH oscillator composed of $CaSO_3$−$H_2O_2$−$NaHCO_3$−$H_2SO_4$ was applied to force the periodic adsorption−desorption of Ag nanoparticles on the gel surface. The experimental conditions for the chemical oscillator were optimized to obtain long-lasting high-amplitude pH oscillations in a closed reactor. The periodic adsorption−desorption was proved to be induced by the periodic pH change in the solution, although the two phenomena were not completely synchronized. That is, the periodic time was longer and the number of oscillations was less for the adsorption−desorption compared with the pH oscillations that occurred in the solution state. However, the heterogeneous oscillations obtained in this study clearly suggested that the hydrophobic interaction was reversibly changed in the patterned pH-responsive hydrogel surface, similar to various biological systems in nature.

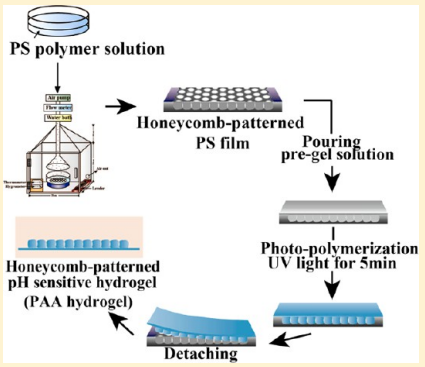


## 1. INTRODUCTION

Several scientists who are interested in the field of polymers have recently focused on smart hydrogels that can undergo large reversible 3D physical or chemical changes in response to small external changes in environmental conditions, such as temperature,[1] pH,[2,3] light intensity,[4] magnetic or electric field,[5] ionic strength,[6] and biological environment.[7]

The hydrogel response mechanism is based on the chemical structure of the polymer network. Among stimuli-responsive hydrogels, pH- and temperature-responsive hydrogels are studied the most because of their potential applications in the biomedical field, such as therapeutic agent delivery systems, tissue engineering scaffolds, cell culture supports, bioseparation devices, sensors, and actuator systems.[8−11]

The pH-responsive polymers are polyelectrolytes with weak acidic or basic groups in their structure that either accept or release protons in response to changes in environmental pH. Temperature-responsive hydrogels are based on polymers that exhibit a lower critical solution temperature (LCST); the gels collapse as the temperature increases. Below LCST, hydrogen bonding between hydrophilic segments of the polymer chain and water molecules is dominant, leading to enhanced dissolution in water. However, as the temperature increases, hydrophobic interactions become strengthened, whereas hydrogen bonding becomes weaker. The net result is shrinking of the hydrogels due to interpolymer chain association through hydrophobic interactions. Poly(*N*-isopropylacrylamide) (PNIPAAm) and NIPAAm copolymers have been the most studied among these systems.[12,13]

Despite great interest in stimuli-responsive polymers or hydrogels for the exploitation of their useful and advanced attributes, such as serving as drug or gene carriers with triggered release properties, the novel functions of responsive polymeric systems have an important role in detection and sensing applications. However, stimuli-responsive polymer-based detection systems are still in their infancy compared with the relatively mature field of small-molecule probes.[14,15] One major limitation of bulk hydrogels for potential applications as stimuli-sensitive hydrogels in detection and sensing systems is the diffusion-rate-limited transduction of signals. However, this limitation can be obviated by engineering interconnected pores in the polymer structure to form capillary networks in the matrix, as well as by downscaling the size of the hydrogel particles to significantly decrease the diffusion paths.[16] More effective applications of such hydrogels require fast response to external stimuli. Thus, to achieve this response, the bulk stimuli-sensitive hydrogel is reduced to small particles because the response rate is inversely proportional to the

**Received:** January 31, 2013
**Revised:** April 23, 2013

   dx.doi.org/10.1021/jp401100z | *J. Phys. Chem. B* XXXX, XXX, XXX−XXX

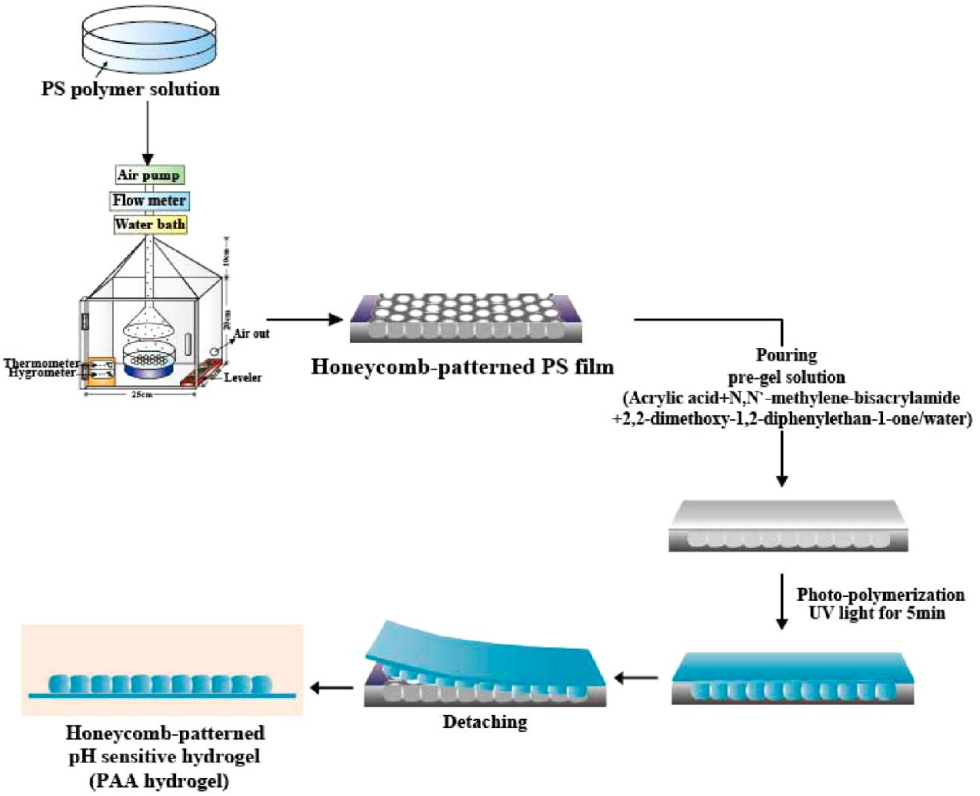


**Figure 1.** Overall experimental procedure for the preparation of a honeycomb-patterned pH-responsive hydrogel surface, which was obtained using the honeycomb-patterned PS film as a template.

square of the characteristic dimension of the hydrogel.[17] Consequently, the preparation of nano- or microsized hydrogel particles[18,19] and the fabrication of stimuli-responsive hydrogels have become very important for potential applications of such materials.[3,20]

An example of these processes is the microfabrication of hydrogel to a patterned hydrogel film that can rapidly respond to external stimuli for the adsorption or desorption of nanoparticles in the hydrogel via increasing the surface area of the film, which can significantly change the pattern structures in the hydrogel film for a greater sensitivity to environmental conditions. The hydrogel film is fabricated using highly ordered honeycomb-patterned porous films as a template prepared through the method introduced by Pitois et al.[21] Highly ordered polymer films are produced by evaporating a polymer solution in a volatile solvent under humid conditions. Water vapor condenses onto the cooling surface due to rapid solvent evaporation. The droplets are then trapped in the solution surface via surface tension.

Hydrophobic interaction has a prominent role in biological processes, such as in lipid bilayer formation,[22] protein folding,[23] and protein−protein recognition.[24] As one of the universally weak interactions in nature, hydrophobic interaction can be observed in smart hydrogel surfaces. Therefore, novel smart surfaces can be designed by utilizing weak hydrophobic interactions to reversibly adsorb and desorb target particles.

An oscillatory stimuli system is expected to be more effective than a single striking stimulus for the reversible adsorption and desorption point of the target particles. Periodic pH oscillations discovered recently in some chemical reactions may be used for periodic stimuli of pH-responsive hydrogels. However, almost all pH oscillations function only under continuous-flow-stirred tank reactor (CSTR) conditions[25] or in a semibatch reactor configuration,[26−28] where all or some of the reagents are continuously supplied into the reactor to keep the system far from chemical equilibrium. These oscillators usually exhibit large amplitudes under such conditions.[29] In the respect of the present application, continuous flow is a significant drawback that is desired to be avoided. However, long-lasting, large-amplitude pH oscillations are not feasibly obtained for the proposed applications due to the lack of continuous inflow of reagents, namely, in a closed reactor.[30,31]

In this study, the oscillations of the adsorption−desorption of nanoparticles on a patterned pH-sensitive hydrogel surface were induced by a newly designed pH oscillatory system occurring in a closed chemical system. The patterned hydrogel surface, whose hydrophobic interaction on silver nanoparticles changes depending on the environmental pH, was fabricated using a highly ordered honeycomb-patterned polystyrene film as a template. Long-lasting, large-amplitude pH oscillations in a closed reactor were obtained via a chemical system of $CaSO_3$−$H_2O_2$−$NaHCO_3$−$H_2SO_4$, designed with a small modification from a recently reported system of $CaSO_3$−$H_2O_2$−$Na_2CO_3$−$H_2SO_4$.[32] Modification was conducted because the $CO_2$ from the air inhibited the long-lasting oscillations. Through the long-lasting periodic pH changes, oscillations of the adsorption−desorption of silver nanoparticles were obtained on the patterned hydrogel surface, indicating that a heterogeneous oscillation was induced by a homogeneous chemical oscillatory system. Moreover, the concentration of silver nanoparticles in the beaker was measured using the circulating UV−vis spectrometer in real time.


dx.doi.org/10.1021/jp401100z | J. Phys. Chem. B XXXX, XXX, XXX−XXX

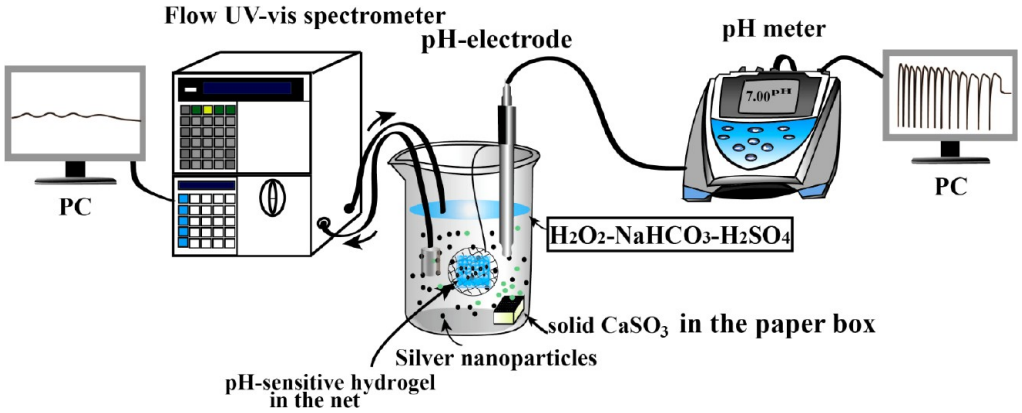


**Figure 2.** Experimental scheme for the simultaneous detection of pH and adsorption−desorption oscillations induced by the pH oscillator in a closed system.

## 2. EXPERIMENTAL SECTION

**2.1. Materials.** Polystyrene (average MW 400 000 g $mol^{-1}$), acrylic acid (99%), *N*,*N*′-methylenebisacrylamide (MBAAm, 99%), 2,2-dimethoxy-1,2-diphenylethan-1-one (Irgacure 651), hydrochloric acid (HCl), sodium hydroxide (NaOH), sodium carbonate ($Na_2CO_3$), sulfuric acid ($H_2SO_4$), hydrogen peroxide ($H_2O_2$, 30%), sodium sulfite ($Na_2SO_3$), calcium chloride ($CaCl_2$), chloroform (99.8%), silver nitrate ($AgNO_3$), acetonitrile (99.8%), and poly(*N*-vinylpyrrolidone) (PVP, average MW 40 000 g $mol^{-1}$) were obtained from Aldrich Co. Tetrathiafulvalene (TTF) was purchased from John Mattey Co. All reagents were used as received without further purification. Deionized water was used in all experimental procedures.

**2.2. Procedures.** *2.2.1. Preparation of a Honeycomb-Patterned pH-Responsive Hydrogel Surface.* The honeycomb-patterned pH-responsive hydrogel film was fabricated via the photopolymerization of acrylic acid on the patterned polystyrene (PS) template films. The detailed procedure for the preparation of the honeycomb-patterned PS thin film was presented in our previous report.[33] A solution of PS in chloroform was cast on a Petri dish and allowed to completely evaporate under humid conditions until an opaque film was obtained. Highly ordered honeycomb-patterned PS films were produced by adding an amphiphilic copolymer ($P_{am}$) to the PS solution. The copolymer was prepared by copolymerization of *N*-dodecylacrylamide and 6-hexaamido acrylic acid.[34]

For the photopolymerization of acrylic acid on the patterned PS template films, acrylic acid (10 g), MBAAm (0.125 g, 0.08 M), and Irgacure 651 (0.256 g, 0.1 M) were dissolved in water as a pregel solution. Photopolymerization was performed in a self-manufactured vacuum chamber. The PS template on the Petri dish was placed in a vacuum chamber, and then, 4 mL of pregel solution was poured on the Petri dish to fabricate a convex-patterned hydrogel film. After removing the air in the vacuum chamber using a vacuum pump for 1 min, the chamber was filled with nitrogen. The mold was then exposed to UV light (Hamamatsu Co. L8252A) for 5 min on the template. The patterned poly(acrylic acid) hydrogel film was prepared by peeling the hydrogel film from the PS template and then rinsing with deionized water. The overall scheme for the preparation of the honeycomb-patterned pH-responsive hydrogel film is summarized in Figure 1.

*2.2.2. pH Responsiveness of the Patterned Hydrogel Surface Morphology.* The patterned PAA hydrogel was poured in three buffer solutions at pH 5, 7, and 9 to compare the morphology with an acidic, neutral, and basic solution, respectively, and to investigate the structural change in response to the variations in environmental pH of the aqueous solution. The convex-patterned gel films equilibrated at a given pH condition were observed using SEM (COXEM CX-100s). The gels were quickly frozen by soaking in liquid nitrogen and lyophilized for 24 h before SEM observation was performed.

*2.2.3. Adsorption−Desorption of Silver Nanoparticles on the Hydrogel Film Depending on the pH by a Hydrophobic Interaction.* Before the oscillation experiments, the pH-responsive adsorptivity of the patterned hydrogel surface was examined using buffer solutions with pH 5, 7, and 9 to compare the hydrophobic interaction of the pH-responsive hydrogel surface at different pH conditions. The patterned PAA hydrogel was soaked in the buffer solutions containing the same concentrations of Ag particles. The change in absorbance facilitated by the adsorbed Ag particles in the buffer solutions was then measured using a flowing UV−vis detector (Hitach L-7400). In addition to the absorbance change for the adsorptivity, the adsorbed Ag particles in different buffer solutions of pH 5 and 9 at similar conditions were investigated with a scanning electron microscope (COXEM-CX100s) equipped with an energy-dispersive X-ray spectroscopy (EDS) analyzer. Ag nanoparticles were prepared by reducing $AgNO_3$ using TTF and PVP, respectively. TTF derivatives act as electron donors and then form stable charge-transfer complexes with various organic and inorganic acceptor species.[35] The procedure for Ag metallization was introduced in our previous report.[36]

*2.2.4. Oscillation of pH in a Closed Chemical System and Adsorption−Desorption Oscillation Induced by a pH Oscillator.* Long-lasting, large-amplitude pH oscillations in a closed system were performed using stock solutions of 0.010 M $NaHCO_3$ and 0.010 M $H_2SO_4$. Solid $CaSO_3{\cdot}2H_2O$ was prepared by mixing 100 mL of 1.0 M $Na_2SO_3$ and 100 mL of 1.0 M $CaCl_2$ aqueous solutions at room temperature. The $CaSO_3{\cdot}2H_2O$ precipitate was filtered and washed with water and acetone, dried at room temperature, and then kept from air in a closed vessel during storage. For the oscillations, 0.25 g of $CaSO_3{\cdot}2H_2O$ and 0.5 mL of $H_2O_2$ were added into 20 mL of distilled water by varying the concentration ratio of $NaHCO_3$ and $H_2SO_4$. The reaction was performed in an ice cold bath at a constant temperature of 10 °C. The oscillating pH was measured using a pH meter (Orion Multimeter Model No. 1219001) with a pH-detecting electrode (Orion


dx.doi.org/10.1021/jp401100z | J. Phys. Chem. B XXXX, XXX, XXX−XXX

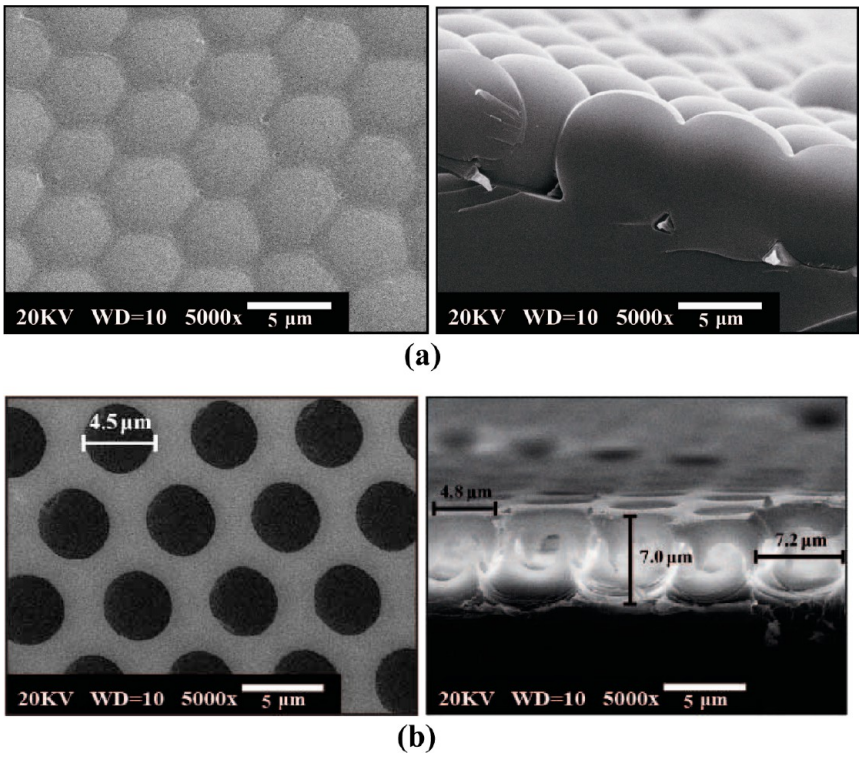


**Figure 3.** (a) Typical SEM image for the honeycomb-patterned PAA hydrogel film and (b) the SEM image of the honeycomb-patterned PS film used for the template of the honeycomb-patterned PAA hydrogel film. The left represents the surface image, and the right represents the cross-sectional image.

8157BNUMD). For the adsorption−desorption oscillations, the patterned hydrogel film cut into 1.0 cm × 1.0 cm × 1.0 mm dimensions was placed in a net and then hung inside of the solution. The oscillations of the adsorption were detected with a flowing UV−vis detector (Hitachi L-7400) at a constant flow rate of 2.0 mL/min. The experimental scheme for the simultaneous detection of pH and adsorption−desorption oscillations induced by the pH oscillator in a closed system is illustrated in Figure 2.

## 3. RESULTS AND DISCUSSION

**3.1. Preparation of a Honeycomb-Patterned Hydrogel Surface.** Figure 3a shows the typical SEM image for the honeycomb-patterned PAA hydrogel film, where the left represents the surface image and the right represents the cross-sectional image. The fabrication of the honeycomb-patterned PAA hydrogel film was performed via the photopolymerization of acrylic acid using MBAAm as a cross-linker and the honeycomb-patterned PS film as the template. Figure 3b shows the SEM image of the honeycomb-patterned PS film used for the template obtained by evaporating the PS solution under humid conditions. The patterned PAA hydrogel film shown in Figure 3a exhibits regularly ordered convex and hexagonal structures, indicating that the experimental method in this study that made use of the template PS film is an effective and facile method for preparing micropatterned hydrogel films. Direct formation of hydrogels with honeycomb-patterned structures by evaporating polymer solutions under humid conditions is impossible because the hydrogel polymer solution is not hydrophobic; a cross-linker should be used in the gelation.

**3.2. pH Sensitivity of the Patterned Hydrogel Surface Morphology.** Figure 4 shows the typical SEM images that indicate the dependency of the surface morphology of the honeycomb-patterned hydrogel surface under various pH conditions, which stimulate the change in the ionization state of the carboxyl group (−$COO^-$/−COOH) included in the PAA hydrogel. Figure 4a−c shows the structure of the patterned hydrogels after 10 min of soaking in the buffer solutions at pH 5, 7, and 9, respectively. A comparison of the SEM images shown in Figure 4a−c indicates that the surface morphology of the hydrogel surface is sensitive to the environmental pH variation of the buffer solutions. The degree of swelling of the hydrogel film surfaces varied. The hexagonal patterns of the PAA hydrogel film after soaking in the buffer solution at pH 5, which is an acid solution, changed into the squeezed state compared with the original structure (Figure 3a), as shown in Figure 4a. The morphology of the patterned hydrogel film after soaking in the neutral buffer solution at pH 7 did not change much from the original state; however, the patterned surface became slightly swollen, as shown in Figure 4b. Meanwhile, the patterned hydrogel after soaking in high-pH buffer solution showed a highly swollen morphology, inducing the deformed or irregularly patterned structure shown in Figure 4c.

A comparison of the SEM images shown in Figure 4a−c indicates that the surface morphology of the hydrogel surface is sensitive to the pH of the buffer solution. A more important result regarding the pH dependency of the surface morphology should be the reversibility of the surface pattern obtained by repeated changes in different pH solutions for the same gel. The reversibility of the pattern morphology and hydrophobic interaction induced by the environmental pH change can be a key issue when considering the application of the hydrogel as a biomimetic smart material. The SEM images shown in Figure 4d indicate the reversibility of surface morphology depending


dx.doi.org/10.1021/jp401100z | J. Phys. Chem. B XXXX, XXX, XXX−XXX

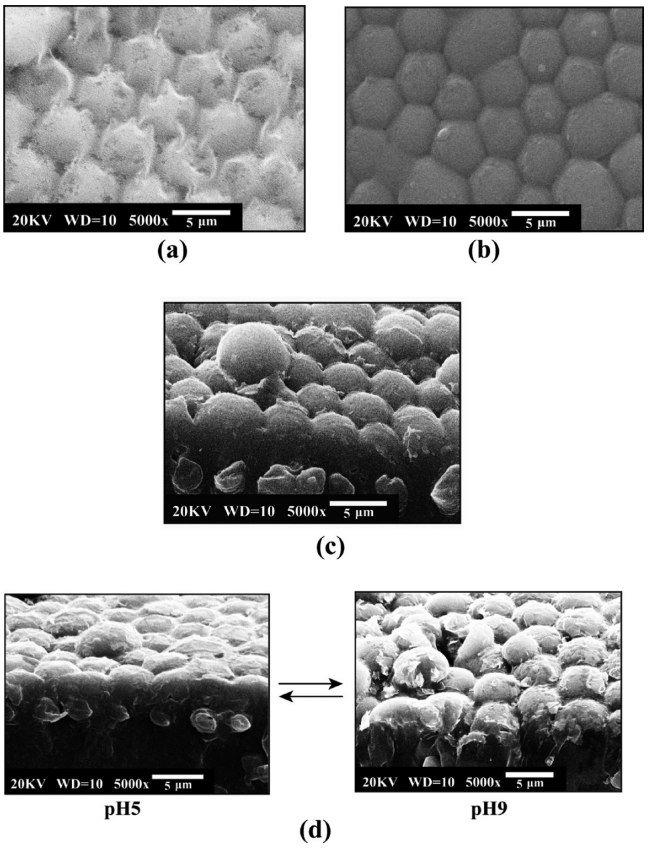


**Figure 4.** Typical SEM images that indicate the dependency of the surface morphology of the honeycomb-patterned hydrogel surface under various pH conditions. Structure of the patterned hydrogels after 10 min of soaking in the buffer solutions at pH (a) 5, (b) 7, and (c) 9. (d) SEM images showing the reversibility of the surface morphology of the patterned hydrogel depending on pH, obtained by alternate soaking of the hydrogel in pH 5 and 9.

on pH. The left and right images were obtained by soaking a hydrogel alternatively in pH 5 and 9 buffer solutions. The left image was obtained at pH 5, whereas the right image was obtained with a pH 9 buffer solution during the repeated process. Although the pattern is not completely the same, a similar structure was recovered with the patterns obtained by the separate buffer solutions of pH 5 and 9, as shown in Figure 4a and c, respectively.

In addition to the morphology change of the gel surface, the adhesion force induced by the hydrophobic interaction should also be changed along with the environmental pH change of the buffer solutions. With a low-pH solution, the equilibrium value for the $[-COO^-]/[-COOH]$ is lower, which induces most of the carboxyl groups in the PAA hydrogel to exist in an un-ionized form. The hydrogen bond between the carboxyl groups may have an important role in the hydrophobic interaction of the hydrogel surface. Therefore, the strong hydrogen bonds interacting in the hexagonal patterns of the PAA hydrogel film acted as important driving forces that squeezed and increased the adhesion force in the patterned hydrogel surface for the adsorption of nanoparticles. However, an ionic repulsion of the ionized carboxyl group induced an electrostatic repulsion force with a high-pH buffer solution, which led to the expansion of the polymeric network. The result thereby attracted more water into the hydrogel network, inducing a more swollen state of the hydrogel surface, which decreased the adhesion force of the nanoparticles through the hydrophilic surface.[37]

**3.3. Adsorptivity of the Hydrogel Surface to Nanoparticles Depending on the pH.** The change in the concentration of the Ag nanoparticles in the aqueous buffer solutions due to the adsorption of Ag nanoparticles on the hydrogel surface was measured using a UV−vis spectrometer to examine the adsorptivity of the patterned PAA hydrogel surface to the nanoparticles existing in the buffer solutions in response to various pH conditions. Figure 5a shows the change of UV−vis absorbance with time at different pH buffer solutions containing Ag nanoparticles. The absorbance wavelength was fixed at 450 nm, which corresponds to the absorbance band of the silver nanoparticles.[38] The absorbance of the solution was decreased in time, indicating that the concentration of the Ag nanoparticles existing in the buffer solutions decreased with time. At the same time, nanoparticles adsorbed on the patterned hydrogel surface from the buffered solution increased simultaneously. Figure 5b shows the difference in the adsorptivity of the hydrogel surface under different buffer solutions by obtaining the value of $[Ag]_{ad}/[Ag]_o$ from the UV−vis absorbance given in Figure 5a, indicating that the adsorptivity of the hydrogel surface was significantly influenced by the pH condition of the environmental buffer solutions. $[Ag]_{ad}/[Ag]_o$ is the ratio of silver nanoparticles adsorbed to the hydrogel surface compared to the initial solution concentration. The equilibrium value of $[Ag]_{ad}/[Ag]_o$ after long-term soaking of the hydrogel surface in the buffer solutions was significantly higher at a lower pH value of 5 than that at pH 9. The adsorption rate (i.e., slope) was also higher in the buffer solution at a lower pH value of 5. The result can be attributed to the hydrophobic interaction of the hydrogel surface induced by the morphological change of the patterned hydrogel surface, as shown in Figure 4. The SEM−EDS image in Figure 5c shows direct evidence of the dependence of the adsorptivity of nanoparticles on the patterned hydrogel surface on the pH. The top image was obtained by soaking a hydrogel film for 10 min in a 0.01 M Ag solution at pH 5, whereas the bottom image was obtained with a pH 9 buffer solution. The Ag peak was higher at pH 5 than that at pH 9, indicating that the adsorptivity is higher at lower pH. The peak of Au seemed to have originated from the coated gold of the SEM image. A strong hydrogen bond interaction in the hexagonal patterns of the PAA hydrogel surface acted as an important driving force that squeezed and increased the adhesion force of the patterned hydrogel surface for the adsorption of nanoparticles.

For reversible adsorption−desorption oscillation, the release rate of the adsorbed silver nanoparticles in different buffer solutions is as important as the adhesion force. Figure 5d shows a comparison of the release rates depending on the pH of the environmental buffer solution. For the experiment, two patterned hydrogels were first soaked in the same beaker containing Ag nanoparticles with neutral water. The release of silver nanoparticles was measured in different beakers with pH 5 and 9 buffer solutions, respectively. The release of adsorbed silver nanoparticles was higher in the higher-pH buffer solution, as shown in Figure 5d, which seems to be a reversed result of the adsorption of nanoparticles on the hydrogel surface shown in Figure 5a. However, this is a reasonable result because the release of adsorbed nanoparticles is slower if the adhesion force of the hydrogel surface is higher.

**3.4. Oscillation of Adsorptivity in the Hydrogel Surface Induced by the pH Oscillations.** Although the


dx.doi.org/10.1021/jp401100z | J. Phys. Chem. B XXXX, XXX, XXX−XXX

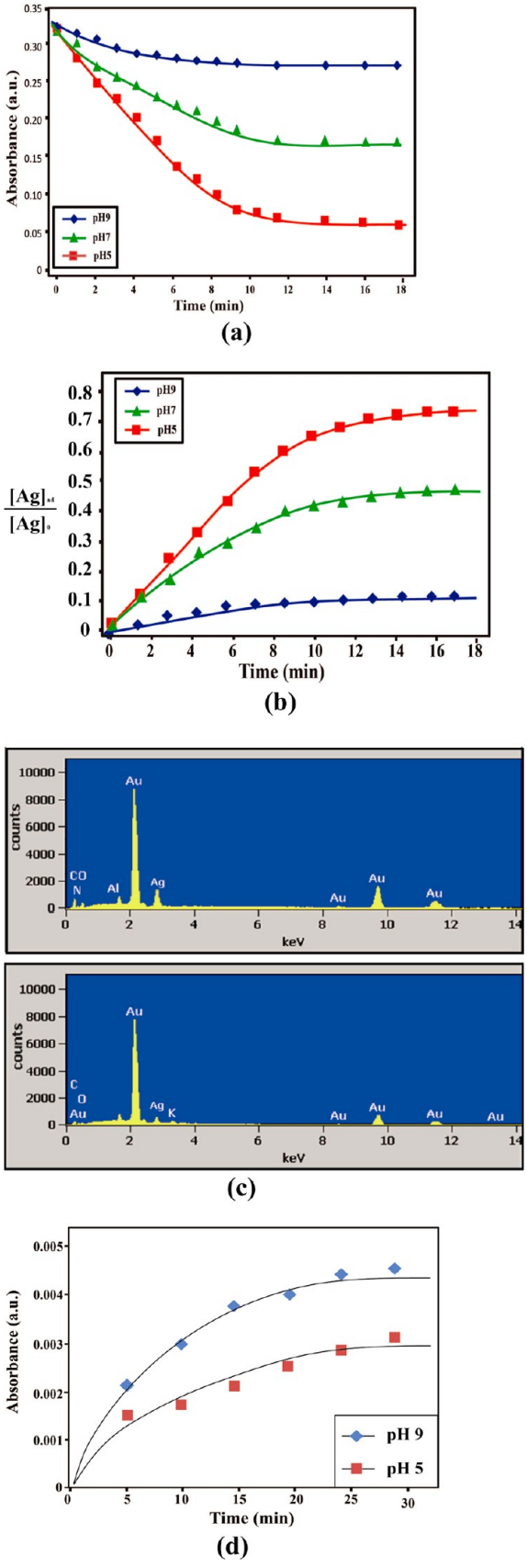


**Figure 5.** Adsorptivity of the hydrogel surface to nanoparticles, depending on pH. (a) The change in UV−vis absorbance with time with different pH buffer solutions containing Ag nanoparticles. (b) Adsorptivity of the hydrogel surface under different buffer solutions by obtaining the value of $[Ag]_{ad}/[Ag]_o$ from the UV−vis absorbance. (c) SEM images showing the difference of adsorbed silver nanoparticles on the hydrogel surface after soaking in different pH buffer solutions. The top image was obtained in pH 5 solution, whereas the bottom image was obtained in pH 9 solution. (d) The release rate depending on pH of the environmental buffer solution, which was first soaked in the same beaker containing Ag nanoparticles with neutral water, and then, the release was measured in different beakers with pH 5 and 9 buffer solutions.

adsorptivity of the hydrogel surface to the Ag nanoparticles was dependent on the pH of the buffer solution, as shown in Figure 5, whether or not a reversible adsorption−desorption of nanoparticles on the hydrogel surface occurs in a periodic variation of pH remains unclear. The pH oscillation occurring in a closed chemical system can prove the possibility of the reversible change of the adsorption−desorption of nanoparticles on the hydrogel surface in an aqueous solution system.

The oscillatory system composed of $CaSO_3$−$H_2O_2$−$NaHCO_3$−$H_2SO_4$ was adopted in this study for pH oscillation in a closed chemical system to induce the reversible change of adsorption−desorption on the patterned hydrogel surface. The system was slightly modified from the recently reported pH oscillatory system of $CaSO_3$−$H_2O_2$−$Na_2CO_3$−$H_2SO_4$[32] because the $CO_2$ from the air inhibited the long-lasting oscillations when $Na_2CO_3$ was used as the initial $HCO_3^-$ source. However, for the system adopted in our study, the obtained pH oscillations were significantly affected by the reaction condition. The temperature should be kept below 10 °C, and the stirring rate should be kept constant at 500 rpm. In addition to the physical condition, the pH oscillations were sensitive to the ratio of $[HCO_3^-]_o/[H_2SO_4]_o$. The dependence of the pH oscillation pattern on the ratio of $[HCO_3^-]_o/[H_2SO_4]_o$ is shown in Figure 6. Figure 6a−f shows that the ratio of $[HCO_3^-]_o/[H_2SO_4]_o$ increased to 0.5, 0.75, 1.0, 1.5, 2.0, and 2.5, respectively. Oscillations were not obtained in higher acidic conditions, where $[HCO_3^-]_o/[H_2SO_4]_o$ corresponded to 0.5, as shown in Figure 6a. However, some oscillation peaks were obtained with high amplitude by increasing the ratio to 0.75, as shown Figure 6b. Long-lasting oscillations were obtained at $[HCO_3^-]_o/[H_2SO_4]_o$ = 1, as shown in Figure 6c, where the oscillations lasted for more than 2000 s with a period length of 2−3 min. However, increasing the ratio to 1.5 and 2.0 decreased the duration of the oscillations, as shown in Figure 6d and e, respectively. The length of the oscillation period was slightly shortened to 1.5 to 2.0 min due to more rapid self-production and consumption of $H^+$. However, oscillations were not obtained when the ratio was further increased to 2.5, as shown in Figure 6f.

The result for the adsorption−desorption oscillations of the nanoparticles induced by the pH oscillations on the hydrogel surface is shown in Figure 7. For the heterogeneous oscillations that occurred on the hydrogel surface, 0.01 M silver nanoparticles with a particle size of about 10 nm were dispersed into the pH oscillatory solution system. The aggregation of the silver particles that inhibit the adsorption−desorption oscillations was not observed in our experimental system. Figure 7a−f shows the result of the oscillations of the adsorption−desorption occurring at the hydrogel surface derived by the conditions given in Figure 6a−f, respectively. Moreover, adsorption−desorption oscillations were not observed at conditions where the pH oscillations were not


dx.doi.org/10.1021/jp401100z | J. Phys. Chem. B XXXX, XXX, XXX−XXX

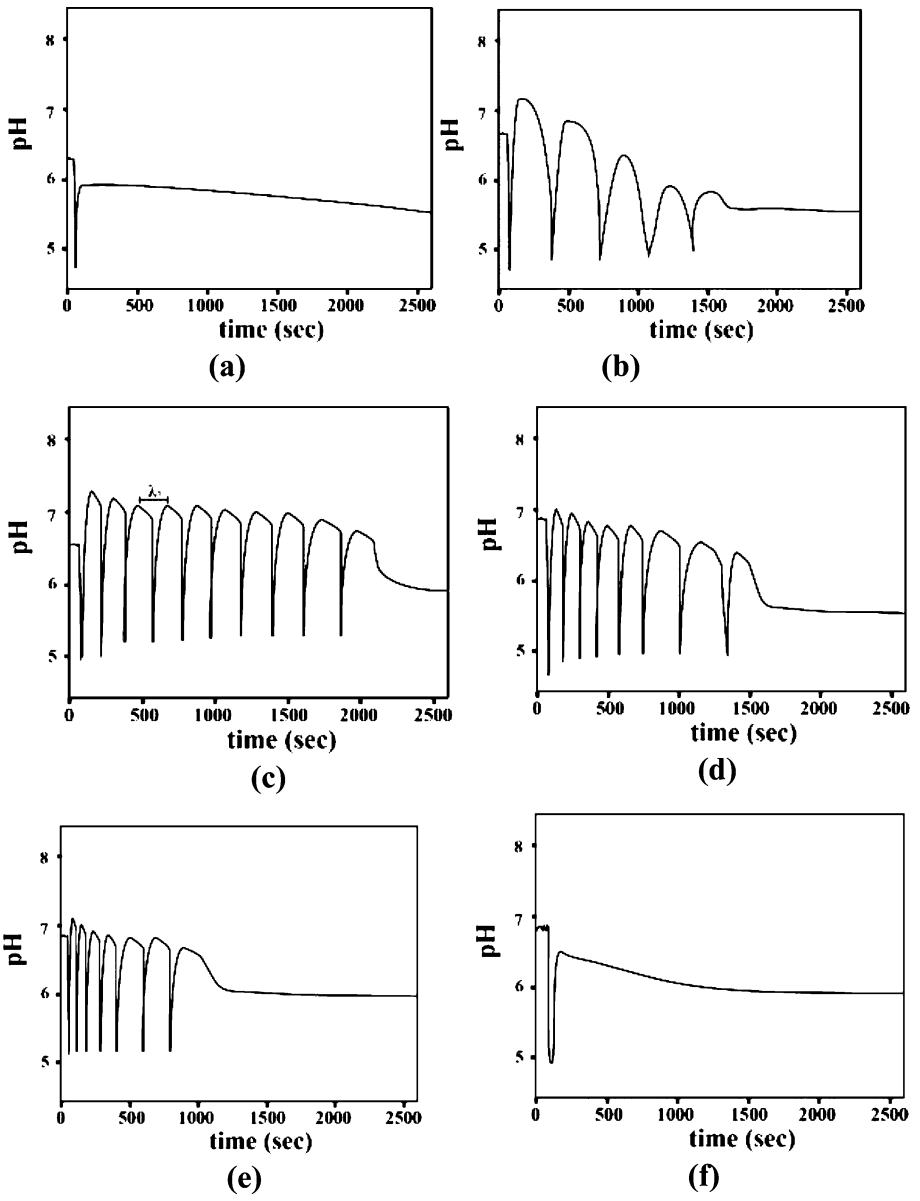


**Figure 6.** Dependence of the pH oscillation pattern on the ratio of $[HCO_3^-]_o/[H_2SO_4]_o$ in the pH oscillatory system of $CaSO_3-H_2O_2-NaHCO_3-H_2SO_4$. $[HCO_3^-]_o/[H_2SO_4]_o$ corresponds to (a) 0.5, (b) 0.75, (c) 1.0, (d) 1.5, (e) 2.0, and (f) 2.5.

obtained, as shown in Figure 7a and f. However, the oscillatory behavior of adsorption−desorption was obtained when the pH oscillations lasted for certain periods, as shown in Figure 7b−d.

In this study, the amplitude of adsorption−desorption oscillations greatly decreased, and the length of the oscillation period ($\lambda_2$) greatly increased compared with that of the pH oscillations ($\lambda_1$). The decrease in amplitude could be due to the difference between the adsorbed and released amount in the same period of soaking time, as shown in Figure 5a and d, respectively. The release was not sensitive to the environmental pH of the buffer solution shown in Figure 5d compared with the adsorption shown in Figure 5a, although the environmental buffer solution had the same pH. The asynchronous oscillating result between the solution oscillation and adsorption−desorption oscillation can be attributed to several factors. One of them is due to the heterogeneous property of the adsorption−desorption oscillation, which differs from the pH oscillations that occur in a homogeneous solution. The nonimmediate response of the hydrogel to the environmental stimuli caused larger average oscillation periods than that of the solution state oscillation, although the patterned hydrogel surface was used to increase the sensitivity. Another reason might be due to the difference between adsorption rate and release rate depending on the environmental pH change, which can cause the decreased sensitivity of the hydrogel surface for the adsorption−desorption oscillations of silver nanoparticles induced by the pH oscillation. Then, silver nanoparticles could be gradually accumulated on the hydrogel surface with oscillation time. In addition to the accumulation of Ag nanoparticles on the hydrogel surface with time, the solid $CaCO_3$ used for the semibatch system inhibited the sensitivity of the hydrogel surface by attaching to the hydrogel surface. The SEM−EDS image shown in Figure 8 well supports the assumption. Figure 8a was obtained from the hydrogel surface in the oscillating solution system after 10 min of soaking, whereas Figure 8b was obtained from the hydrogel surface after 30 min of soaking in the oscillating solution. Both peaks of Ag and Ca increased with the increase in oscillation time. The


dx.doi.org/10.1021/jp401100z | J. Phys. Chem. B XXXX, XXX, XXX−XXX

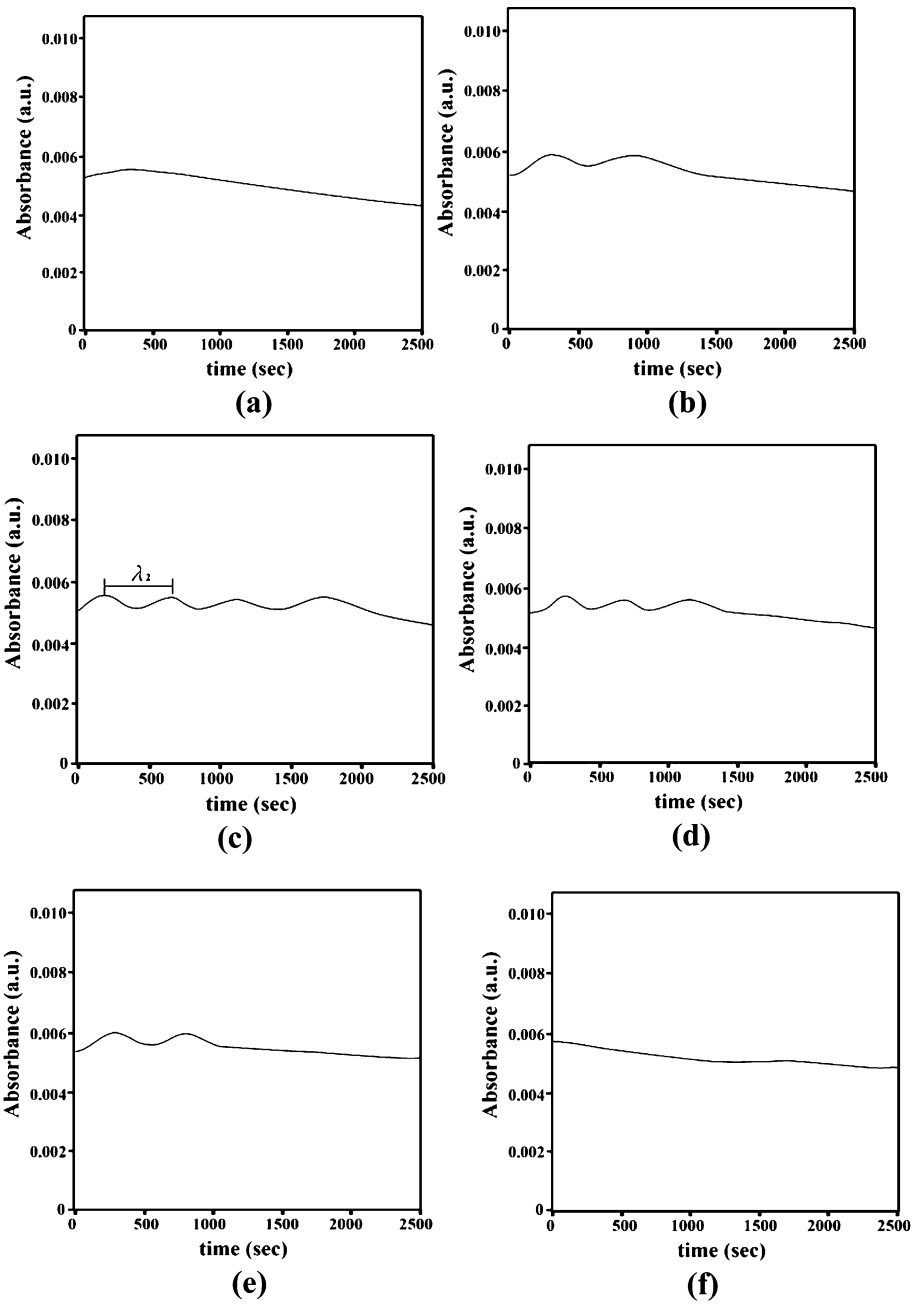


**Figure 7.** Oscillations of the adsorption−desorption occurring at the hydrogel surface derived by the pH oscillations given in Figure 6. The experimental conditions for (a−f) are the same conditions used in Figure 6a−f, respectively.

decrease in the sensitivity of the hydrogel can be the reason why more than four periodic peaks in the oscillations of the adsorption−desorption in our study were not easily obtained.

The oscillations of the adsorption−desorption of silver nanoparticles on the patterned hydrogel surface induced by the pH oscillation in a closed chemical system suggest that the hydrophobic interaction highlighted by the patterned surface of the pH-responsive hydrogel reversibly varied with the environmental pH change.

## 4. CONCLUSIONS

Self-oscillations of the adsorption−desorption of nanoparticles on the hydrogel surface were derived using a pH oscillator occurring in a closed chemical system. The hexagonal patterns of the PAA hydrogel surface were changed to a squeezed structure in lower-pH buffer solutions, whereas the patterned surface became highly swollen with deformed or irregular structure. In addition to the morphology change of the surface, the equilibrium value of $[Ag]_{ad}/[Ag]_o$ at long periods of soaking of the hydrogel surface in the buffer solutions was significantly higher in a lower-pH solution than that in a higher-pH solution.

The oscillatory system composed of $CaSO_3-H_2O_2-NaHCO_3-H_2SO_4$ was adopted in this study for the pH oscillation in a closed chemical system, which induced adsorption−desorption oscillations of the nanoparticles on the hydrogel surface. However, for the heterogeneous oscillations, the period of oscillation was significantly higher at 8−10 min, whereas the duration of pH oscillation was 2−3 min. Therefore, the number of oscillations also significantly


dx.doi.org/10.1021/jp401100z | J. Phys. Chem. B XXXX, XXX, XXX−XXX

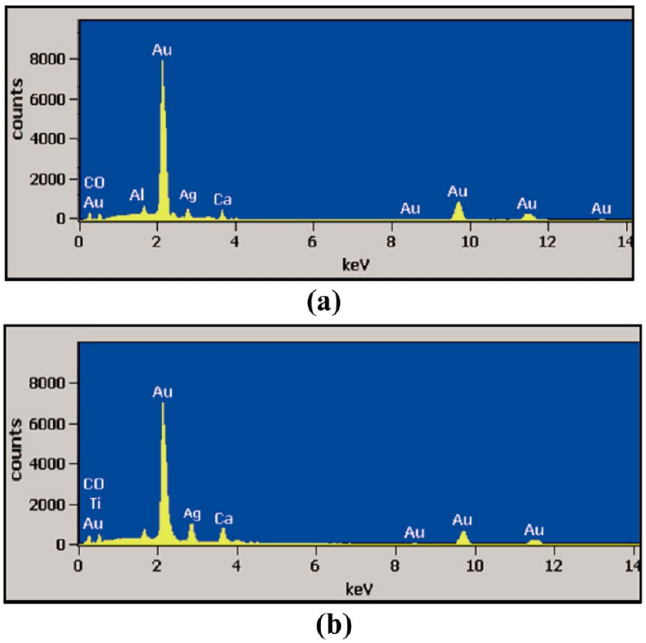


**Figure 8.** SEM–EDS image of the hydrogel surfaces in the oscillating reaction solution obtained at different times of soaking, (a) 10 and (b) 30 min.

decreased compared with the pH oscillations that occurred in the solution state. However, the heterogeneous oscillations obtained in this study clearly suggested that the hydrophobic interaction was reversibly changed in the patterned pH-sensitive hydrogel surface as a biomimetic system.

A further study of the possible governing role of pH oscillators in the reversible adsorption–desorption of nanoparticles on gel surfaces may focus on the use of a pH oscillator with a longer periodic time. In such case, the response time of the gel surface and the period length of the chemical oscillator would be easier to synchronize. A recently reported batch-like pH oscillator[28] seems to meet this expectation. In this case, the key components ($SO_3^{2-}$, $H^+$) of the chemical oscillator are trapped in silica gel, and the continuous supply of the key components during oscillation is provided by the gel. According to the experiments, the period can vary on a large scale. Moreover, an interesting question arises on whether or not the components of the chemical oscillator can be trapped in the gel used in the adsorption–desorption process. Further experiments are needed to answer these questions.

## AUTHOR INFORMATION

### Corresponding Author

*E-mail: chemhds@inje.ac.kr. Tel: 82-55-320-3225. Fax: 82-55-321-9718.

### Notes

The authors declare no competing financial interest.

## ACKNOWLEDGMENTS

This research was supported by the National Research Foundation of Korea and funded by the Ministry of Education, Science, and Technology (NRF) (2012-0007192).

## REFERENCES

(1) Ding, Z.; Chen, G.; Hoffman, A. S. Unusual Properties of Thermally Sensitive Oligomer–Enzyme Conjugates of Poly(N-isopropylacrylamide)-trypsin. *J. Biomed. Mater. Res.* **1998**, *9*, 498–505.
(2) Stayton, P. S.; Shimoboji, T.; Long, C.; Chilkoti, A.; Chen, G. H.; Harris, J. M.; Hoffman, A. S. Control of Protein–Ligand Recognition Using a Stimuli-Responsive Polymer. *Nature* **1995**, *378*, 472–474.
(3) Hu, Z.; Chen, Y.; Wang, C.; Zheng, Y.; Li, Y. Polymer Gels with Engineered Environmentally Responsive Surface Patterns. *Nature* **1998**, *393*, 149–152.
(4) Hrouz, J.; Ilavský, M.; Ulbrich, K.; Kopěc, J. The Photoelastic Behaviour of Dry and Swollen Networks of Poly(N,N-diethylacrylamide) and of its Copolymers with N-tert-Butylacrylamide. *Eur. Polym. J.* **1981**, *17*, 361–366.
(5) Kwon, I. C.; Bae, Y. H.; Kim, S. W. Electrically Erodible Polymer Gel for Controlled Release of Drugs. *Nature* **1991**, *354*, 291–293.
(6) Kokufuta, E.; Tanaka, T. Biochemically Controlled Thermal Phase Transition of Gels. *Macromolecules* **1991**, *24*, 1605–1607.
(7) Suzuki, A.; Tanaka, T. Phase Transition in Polymer Gels Induced by Visible Light. *Nature* **1990**, *346*, 345–347.
(8) Packhaeuser, C. B.; Schnieders, J.; Oster, C. G.; Kissel, T. J. In Situ Forming Parenteral Drug Delivery Systems: An Overview. *Eur. Pharm. Biopharm.* **2004**, *58*, 445–455.
(9) Hatefi, A.; Amsden, B. Biodegradable Injectable in Situ Forming Drug Delivery Systems. *J. Controlled Release* **2002**, *80*, 9–28.
(10) Jeong, B.; Bae, Y. H.; Kim, S. W. Biodegradable Block Copolymers As Injectable Drug-Delivery Systems. *Nature* **1997**, *388*, 860–862.
(11) Jeong, B.; Gutowska, A. Lessons from Nature: Stimuli-Responsive Polymers and Their Biomedical Applications. *Trends Biotechnol.* **2002**, *20*, 305–311.
(12) Hoffman, A. S.; Affrassiabi, A.; Dong, L. C. Thermally Reversible Hydrogels: II. Delivery and Selective Removal of Substances from Aqueous Solutions. *J. Controlled Release* **1986**, *4*, 213–222.
(13) Bae, Y. H.; Okano, T.; Hsu, R.; Kim, S. W. Thermo-Sensitive Polymers As On–Off Switches for Drug Release. *Macromol. Rapid Commun.* **1987**, *8*, 481–485.
(14) Cho, D. G.; Sessler, J. L. Modern Reaction-Based Indicator Systems. *Chem. Soc. Rev.* **2009**, *38*, 1647–1662.
(15) Basabe-Desmonts, L.; Reinhoudt, D. N.; Crego-Calama, M. Design of Fluorescent Materials for Chemical Sensing. *Chem. Soc. Rev.* **2007**, *36*, 993–1017.
(16) Chaterji, S.; Kwon, I. K.; Park, K. Smart Polymeric Gels: Redefining the Limits of Biomedical Devices. *Prog. Polym. Sci.* **2007**, *32*, 1083–1122.
(17) Tanaka, T.; Fillmore, D. J. Kinetics of Swelling of Gels. *J. Chem. Phys.* **1979**, *70*, 1214–1218.
(18) Kuckling, D.; Vo, C. D.; Wohlrab, S. E. Preparation of Nanogels with Temperature-Responsive Core and pH-Responsive Arms by Photo-Cross-Linking. *Langmuir* **2002**, *18*, 4263–4269.
(19) Kuckling, D.; Vo, C. D.; Adler, H. J. P.; Volkel, A.; Colfen, H. Preparation and Characterization of Photo-Cross-Linked Thermosensitive PNIPAAm. *Macromolecules* **2006**, *39*, 1585–1591.
(20) Beines, P. W.; Klosterkamp, I.; Menges, B.; Jonas, U.; Knoll, W. Responsive Thin Hydrogel Layers from Photo-Cross-Linkable Poly(*N*-isopropylacrylamide) Terpolymers. *Langmuir* **2007**, *23*, 2231–2238.
(21) Pitois, O.; Francois, B. Crystallization of Condensation Droplets on a Liquid Surface. *Colloid Polym. Sci.* **1999**, *277*, 574–578.
(22) Engelman, D. M. Membranes Are More Mosaic than Fluid. *Nature* **2005**, *438*, 578–580.
(23) Tanford, C. The Hydrophobic Effect and the Organization of Living Matter. *Science* **1978**, *200*, 1012–1018.
(24) Janda, C. Y.; Li, J.; Oubridge, C.; Hernandez, H.; Robinson, C. V.; Nagai, K. Recognition of a Signal Peptide by the Signal Recognition Particle. *Nature* **2010**, *465*, 507–510.
(25) Rabai, G.; Orban, M.; Epstein, I. R. Systematic Design of Chemical Oscillators. 64. Design of pH-Regulated Oscillators. *Acc. Chem. Res.* **1990**, *23*, 258–263.

(26) Rabai, G.; Epstein, I. R. Systematic Design of Chemical Oscillators. 80. pH Oscillations in a Semibatch Reactor. *J. Am. Chem. Soc.* **1992**, *114*, 1529−1530.
(27) Rabai, G.; Kaminaga, A.; Hanazaki, I. The Role of the Dushman Reaction and the Ferricyanide Ion in the Oscillatory $IO^{-3}$−$SO_2^{-3}$−$Fe(CN)_4^{-6}$ Reaction. *J. Phys. Chem.* **1995**, *99*, 9795−9800.
(28) Poros, E.; Horvath, V.; Kurin-Csorgei, K.; Epstein, I. R.; Orban, M. Generation of pH-Oscillations in Closed Chemical Systems: Method and Applications. *J. Am. Chem. Soc.* **2011**, *133*, 7174−7179.
(29) Kovács, K. M.; Rábai, G. Large Amplitude pH Oscillations in the Hydrogen Peroxide−Dithionite Reaction in a Flow Reactor. *J. Phys. Chem.* **2001**, *105*, 9183−9187.
(30) Giannos, S. A.; Dinh, S. M.; Berner, B. Temporally Controlled Drug Delivery Systems: Coupling of pH Oscillators with Membrane Diffusion. *J. Pharm. Sci.* **1995**, *84*, 539−543.
(31) Liedl, T.; Simmel, F. C. Switching the Conformation of a DNA Molecule with a Chemical Oscillator. *Nano Lett.* **2005**, *5*, 1894−1898.
(32) Rábai, G. pH-Oscillations in a Closed Chemical System of $CaSO_3$−$H_2O_2$−$HCO_3^-$. *Phys. Chem. Chem. Phys.* **2011**, *13*, 13604−13606.
(33) Kim, B. S.; Basavaraja, C.; Jo, E. A.; Kim, D. G.; Huh, D. S. Effect of Amphiphilic Copolymer Containing Ruthenium Tris-(bipyridyl) Photosensitizer on the Formation of Honeycomb-Patterned Film. *Polymer* **2010**, *51*, 3365−3371.
(34) Yabu, H.; Shimomura, M. Simple Fabrication of Micro Lens Arrays. *Langmuir* **2005**, *21*, 1709−1711.
(35) Roncali, J. Linearly Extended p-Donors: When Tetrathiafulvalene Meets Conjugated Oligomers and Polymers. *J. Mater. Chem* **1997**, *7*, 72307−72321.
(36) Kim, J. K.; Basavaraja, C.; Yamaguchi, T.; Huh, D. S. Preparation and Characterization of Smart Hydrogel Nanocomposites Sensitive to Oxidation−Reduction. *Polym. Bull.* **2013**, *70*, 207−220.
(37) Zhao, S.; Cao, M.; Wu, J.; Xu, W. Synthesis and Characterization of Biodegradable Thermo- and pH-Sensitive Hydrogels Based on Pluronic F127/Poly(ε-caprolactone) Macromer and Acrylic Acid. *Macro. Res.* **2009**, *17*, 1025−1031.
(38) Šileikaite, A.; Prosycevas, I.; Puiso, J.; Juraitis, A.; Guobiene, A. Analysis of Silver Nanoparticles Produced by Chemical Reduction of Silver Salt Solution. *Mater. Sci.* **2006**, *12*, 287−291.